

# 6

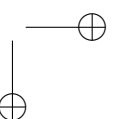
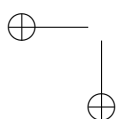
## MAPPING OF OVERBURDEN SUBSTRATES FOR MINE SITE RE-CULTIVATION

*Jan Frouz, Miroslav Píkl, Olga Vindušková, and František Zemek*

### 6.1 Introduction

Open pit coal mining has a severe impact on ecosystems in the mining area. An ecosystem affected by opencast mining is literally erased, either excavated or buried. Overburden (spoil) overlying the coal seam is removed and deposited in heaps leading to disruption of large areas (Bell & Donnelly, 2006). In many cases, overburden material becomes the parent substrate for soil development (Šourková et al. 2005; Karu et al. 2009).

This overburden material comes often from large depth, often over hundred meters. These substrates differ substantially from recent soils. They often have extreme pH (too acidic or too alkaline), extreme texture (gravel, sandy or clay), and in many cases the material is separated in terms of grains of similar size. In some locations overburden material may contain high concentrations of heavy metals and or may have high salt content reflected in high conductivity. The substrates often lack recent organic matter but may contain fossil organic matter of



various origin (Bradshaw 1997).

Contrary to other polluted sites where toxicity appears as a result of the accumulation of exogenous toxic substances, in post-mining sites the toxicity is typically a result of in situ weathering. Weathering, namely pyrite oxidation, decreases pH and may release heavy metals. Weathering may also release other ions that may cause high conductivity of the substrate resulting in toxicity of post mining sites (Bradshaw 1997; Frouz et al. 2005). Determination of potential toxicity of post mining sites is important for prediction of their future development. For example in Sokolov coal mining district in nontoxic sites, vegetation coverage can be reached by proper reclamation in 5-10 years and even spontaneous succession processes lead to vegetation cover in 10–15 years (Frouz et al. 2014), whereas in sites with high pyrite oxidation, vegetation may not appear for next 50 years (Frouz et al. 2014).

Biological tests with overburden material show that its toxicity in Sokolov area is most closely associated with pH, conductivity and polyphenol content. Primary cause of pH decrease is usually pyrite weathering. Pyrite in coal mining sites is usually associated with the coal seam; consequently, toxicity problems are typically the most severe in substrates that contain traces of coal. Identification of coal may thus be a good indicator of toxicity. This effect may be enhanced in materials with low sorption capacity, and low content of basic cations such as in sand or kaolinite. Besides toxicity associated with coal accompanied by pyrite, there may be also other mechanisms causing toxicity, e.g., sites with high conductivity given by high content of carbonates and sulfates may be toxic for plants and soil fauna due to high osmotic pressure (Frouz et al. 2005).

Identification of fossil organic matter (FOM) and characterizing its quality may be important in identifying potentially toxic sites. After reclamation or during spontaneous recovery of the vegetation cover, the content of recent soil organic matter (RSOM) gradually increases (Šourková et al. 2005). This has positive impacts on soil quality (increases porosity, aeration, water capacity of soil and infiltration). RSOM also represents an energy and nutrient source for soil biota (Brady & Weil 1999); moreover, RSOM represents a carbon sink and may reduce the rising concentration of CO<sub>2</sub> in the atmosphere (IPCC 2007).

The amount of RSOM in soils is determined as organic carbon content. However, in mine soils fossil forms of organic carbon such as coal or kerogen can also be frequently found (Vindušková & Frouz 2013). Conventional methods for soil organic carbon determination unfortunately cannot distinguish between recent and fossil carbon forms. The only method suitable for such differentiation is radiocarbon dating. However, this method is very expensive, thus it cannot be used routinely. Proximal remote sensing techniques such as near infrared spectroscopy (NIRS) hold potential to discriminate between recent and fossil carbon forms.

In general, remote sensing techniques are useful in the study of many soil properties (Ben-Dor et al. 1997; Mulder et al. 2011). However, a common problem with the study of soil properties using airborne devices is that soil is

often covered by vegetation and if the soil is bare, the surface layer of the soil is often covered by physical or biological crusts that may have different properties than deeper soil horizons. In this aspect, post mining areas are ideally suited for using remote sensing tools as they have a large area of bare soil which often was quite recently homogenized during the heaping process. Moreover, for many key processes such as erosion or plant establishment, the conditions of the surface layer are more important than conditions in deeper soil.

In this chapter, we illustrate the possible application of remote sensing techniques to map post mining substrates having various types of potential toxicity or even to directly predict the toxicity of post mining sites and estimate content of fossil and recent organic matter.

## 6.2 Material and Methods

### 6.2.1 Study Area

Two set of post mining sites were used in this study. The first set consists of 42 sites described in (Frouz et al. 2005). These were sampled in three mining districts: 1. Sokolov – coal-mining district near the towns Sokolov and Chodov (North-West Czech Republic), 2. North Czech coal mining district near Bílina and Ústí nad Labem (North Bohemia), and 3. Lusatian mining district near Cottbus (Eastern Germany). Both Czech areas are brown coal mining district whereas lignite is mined in Germany near Cottbus. In all sites, open cast mines produce large areas of tailings where spoil material was sampled. In both Czech coal-mining districts, claylike tertiary sediments dominated, whereas sand was most frequent in German mining district. This set was used for comparison of chemical and ecotoxicological characterization of substrates with laboratory spectral measurements.

The second set of plots was located in post mining plots near Sokolov (Czech Republic). Average altitude of the study area is about 500—700 m a.s.l. In majority of the heaps, the overburden consists mainly of tertiary clays of Cypris series with alkaline pH. These clays are dominated by kaolinite, illite and montmorillonite, and contain 2–10 % of fossil organic matter. In smaller extent, other substrates are present, namely neutral or slightly acidic tuffites, which are weathered, volcanic ashes of tertiary origin underlying the coal seams, acidic clay substrates dominated with kaolinite, coal and acidic coal rich kaolinite clays, and finally jarosite crusts on tertiary clay substrates. This set, covering a part of the heap of an area about 0.5 ha, was used for comparison of chemical and ecotoxicological characterization of substrates with field measurements of spectra, along with the first set. In addition, this set was used for classification of substrates based on airborne hyperspectral data. In this part of the heap, substrates were mapped by field survey and pH was measured in a regular  $25 \times 25$  m grid.

### 6.2.2 Laboratory Chemical and Ecotoxicological Characterization of Substrates

The material for chemical analysis was air-dried and stored in a dark place at room temperature. Soil pH in water was measured using a pH meter with glass electrode, conductivity was measured in filtrated 1:5 spoil water suspension using a conductometer. Two ecotoxicity tests were applied, i.e., germination of plant *Sinapis alba* and enchytraeid toxicity test. *S. alba* germination was tested with a pot experiment similar to that used by Fargasová (Fargasová 1994; Fargasová 1998). The test is based on proportion of seeds that germinate on given substrate. The enchytraeid toxicity test was conducted as described by Frouz et al. (Frouz et al. 2005); this test measures growth of population of potworms in individual substrates from constant number of introduced even-aged potworms.

### 6.2.3 Spectral Data

#### A. Laboratory spectral measurements

Spectral signatures of 42 clay substrates collected at the first site were measured in a laboratory. The samples were dried and sieved through 2 mm calibrated sieve. The samples were measured in black Petri dishes with ASD FieldSpec 3: spectral range 350–2500 nm, sampling step 1 nm, full width at maximum half – FWHM 3 nm. The Petri dishes with soil samples were placed on a turntable (ASD Inc.) ensuring that measured spectra were homogenized (average of 50 measurements) and all samples were measured with the same viewing and illuminating geometry. White reference panel (Spectralon®) was used to obtain reflectance data directly. Measured spectra were corrected using dynamic, parabolic linear transformation (Beal & Eamon 2009) in order to compensate the shifts between visible and infra-red regions.

To generate a model relating laboratory spectral data with substrate pH or toxicity, two steps were used. In the first step, the correlations between reflectance of substrates at individual wavelengths and pH and toxicity were calculated. Then we identified all local correlation minima or maxima as a function of wavelength. From these, we selected individual wavelengths or mean wavelengths for a certain interval if correlation formed a rather flat plateau. These values were then the subject of multiple regression analysis with forward selection in Statistica 10.

#### B. Field spectral measurements

Field reflectance measurements (ASD FieldSpec 3) of nine substrates were carried out at 14 homogenous plots in the second test area (Sokolov region). We used the white reference panel (Spectralon®) before and after each substrate measurements to obtain directly surface reflectance signatures. The parabolic linear transformation was carried out on measured spectra.



Each plot spectrum was calculated as an average of about 15 individual measurements as some measurements were identified as outliers. ASD measurements were resampled to fit the spectral resolution of the hyperspectral airborne data described in the next section.

### *C. Airborne spectral measurements*

Airborne hyperspectral data over the second site (Sokolov region) were acquired on August 6th 2008 using AISA Eagle pushbroom hyperspectral system with spatial resolution 0.4 m, spectral resolution of 10 nm within spectral range of 400–1000 nm. Ancillary field data were collected simultaneously with the overflight. Field data supported atmospheric and geometric corrections of airborne images (see Section 2.3 for details).

We used CaliGeo (Spectral Imaging Ltd.) software to carry out the radiometric corrections and orthorectification of the raw AISA Eagle image data. ATCOR-4 software was applied for atmospheric, topographic and BRDF corrections of airborne data.

#### **6.2.4 Mapping of Clay Substrate Composition**

We used spectral angle mapper classifier (SAM) to classify soil substrates from the hyperspectral image. SAM is a method for comparing imagery spectra to a spectrum representing the class (Kruse et al. 1993). Training spectra for individual substrate classes were taken from the field ASD measurements described in 6.2.3. The SAM classification was implemented in ENVI using a multiple threshold option. A threshold value was set up for each substrate class. The regions of interest (ROI) were determined based on the known positions of substrates in the area and average value of spectral angle was calculated for a given ROI.

#### **6.2.5 Fossil Organic Matter Characterization Using Near Infrared Spectroscopy**

Near infrared spectra were laboratory measured in a spectral range from 1000 to 2500 nm. Artificial mixtures ( $n = 125$ ) of claystone, coal and recent organic matter (from fermentation layer) were measured as well as a set of 14 soils in which recent carbon was previously determined by radiocarbon dating (Karu et al. 2009). The recent carbon content in mixtures was calculated from the proportion of recent organic matter and its total organic carbon content. The total organic carbon content in mixtures was calculated as a sum of organic carbon from claystone, coal and recent organic matter.

Partial least squares (Janik et al. 2007) was used to develop calibration models between reflectance and total organic carbon (C<sub>tot</sub>) and recent carbon (C<sub>rec</sub>) content — first using only the mixtures, then adding also the soil spectra.

## 6.3 Results and Discussion

### 6.3.1 Spectral Signatures of Different Clay Substrates Measured in a Lab and Their Relation to Chemistry and Toxicity

Earlier studies (Frouz et al. 2005; Frouz et al. 2011) show that conductivity and pH are major factors contributing to substrate toxicity for representatives of both soil fauna and plants. Using multiple regressions with forward selection, we were able to produce an equation that predicts pH of overburden from laboratory spectroscopic data (Figure 6.1) obtained in three mining sites (Table 6.1). Despite the fact that this approach was very successful in determining pH (the equation is highly significant and explains more than 80 % of data variability), the attempt to explain toxicity the same way was much less successful. Although the resulting equation was also statistically significant it explained only 23 % of data variability. This discrepancy between successful estimate of pH and less successful estimate of toxicity is caused by fact that the toxicity of post-mining sites is quite complex as several environmental factors and their combinations contribute to the final toxicity of the substrate (Frouz et al. 2005; Frouz et al. 2011). The most frequent reason for the toxicity is a low pH. Low pH also increases the solubility of aluminium and other metals which may contribute to the toxicity of substrates. This indicates that the effect of pH may be modified by the presence of metals, namely As. High conductivity caused by the high concentration of cations, namely Na, is another reason for high toxicity. The high conductivity is sometimes accompanied by a high pH. Finally, toxicity is often accompanied by coal, as coal content closely negatively correlates with pH but potentially may affect soil biota also directly through polyphenols in coal (Frouz et al. 2005). This complexity of toxicity is a reason why the attempt to estimate toxicity as a simple function of spectral properties did not meet with much success.

### 6.3.2 Spatial Distribution of Clay Substrates Using AISA Eagle Images and Their Use for Prediction of Toxicity

Geological substrates forming the overburden have similar chemical properties and toxicity values (Frouz et al. 2005) and are often distinct from other substrates. Because toxicity is very complex problem, as was explained above, it seems to be more promising to use hyperspectral data to classify prevailing overburden substrate and then estimate potential toxicity based on mean values of toxicity for individual overburden substrates. Classification of individual overburden substrate types from airborne hyperspectral data was done using spectral angle mapper. Overall classification accuracy was 71.18 %. Classification results for each substrate are presented in Table 6.2. Clay substrates of the Cypris series were divided for the purpose of classification into yellow and grey subclass. Both dominate the area and these subclasses reached the highest classification accuracy.

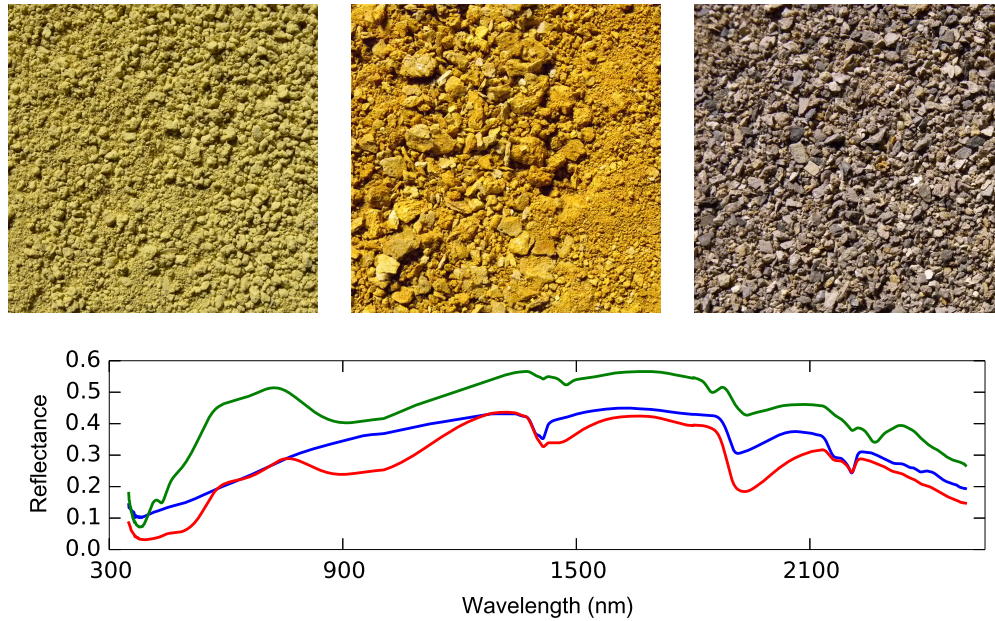


**Figure 6.1** Samples and spectra of selected clay substrates: Top left image, green line in plot above – yellow clay (illite + jarosite). Top middle, red line – jarosite crust. Top right, blue line – coal clay (kaolinite + coal)

This classification was then used to produce a map of substrates in about one ha area of Podkrušňohorská heap with large variety of substrates (Figure 6.2). In this area, 14 samples were randomly taken and their toxicity was tested by *Sinapis alba* germination test. The combination of average substrate toxicity with the substrate map obtained from hyperspectral data gives us spatial prediction of substrate toxicity. Comparison of toxicity predicted using hyperspectral data and measured toxicity in these 14 points indicates that predictions of substrate toxicity using hyperspectral data with substrate classification explains about 55 % of data variability. This is greater than toxicity as predicted on basis of pH value extrapolated from regular grid of points, which explains only 21 % of data variability.

The reason why hyperspectral mapping is much more successful in this context is connected with the manner in which the heap was created. Individual piles of material of different origin are heaped in various shapes and in sizes which are below the resolution of the  $25 \times 25$  m grid. Edges of these piles are very narrow and basically unpredictable by classical interpolation techniques.

**Table 6.1** Results of multiple regression estimating substrate (a) pH and (b) toxicity based on laboratory hyperspectral data.

| a) | Wavelength | Coefficient | SD <sup>a</sup> | p <sup>a</sup> |
|----|------------|-------------|-----------------|----------------|
|    | intercept  | 9.46        | 0.95            | < 0.0001       |
|    | 1270       | -247.23     | 156.80          | 0.1241         |
|    | 435–450    | 88.59       | 13.67           | < 0.0001       |
|    | 380–385    | -105.61     | 18.59           | < 0.0001       |
|    | 350        | -7.94       | 9.10            | 0.3891         |
|    | 1880–1885  | 76.09       | 11.84           | < 0.0001       |
|    | 1425–1430  | -106.47     | 17.97           | < 0.0001       |
|    | 1249       | 265.60      | 160.15          | 0.1064         |

| b) | Wavelength | Coefficient | SD <sup>a</sup> | p <sup>a</sup> |
|----|------------|-------------|-----------------|----------------|
|    | intercept  | 0.76        | 0.23            | 0.0024         |
|    | 1290       | -2.00       | 0.62            | 0.0026         |
|    | 435–450    | 7.09        | 3.47            | 0.0481         |
|    | 380–385    | -6.48       | 4.33            | 0.1427         |

<sup>a</sup> SD – standard deviation, p – probability

**Table 6.2** Classification accuracies for overburden substrates in Podkrušňohorská post mining heap near Sokolov.

| Substrate                         | Producer accuracy <sup>a</sup> [%] | User accuracy <sup>b</sup> [%] |
|-----------------------------------|------------------------------------|--------------------------------|
| coal clay                         | 97.76                              | 51.82                          |
| clay of cypris series<br>– yellow | 100.00                             | 99.76                          |
| tuffites                          | 48.85                              | 100.00                         |
| kaolinitic clays                  | 76.49                              | 99.48                          |
| underlying soils                  | 27.27                              | 25.53                          |
| clay of cypris series<br>– grey   | 93.42                              | 85.34                          |
| coal with clay                    | 50.00                              | 97.40                          |
| coal                              | 60.89                              | 100.00                         |
| Jarosite cover on clay            | 49.02                              | 100.00                         |

<sup>a</sup> Producer accuracy results from dividing the number of correctly classified pixels in each class by the number of training pixels used for that class.

<sup>b</sup> User accuracy results from dividing the number of correctly classified pixels in each category by the total number of pixels that were classified in that class.

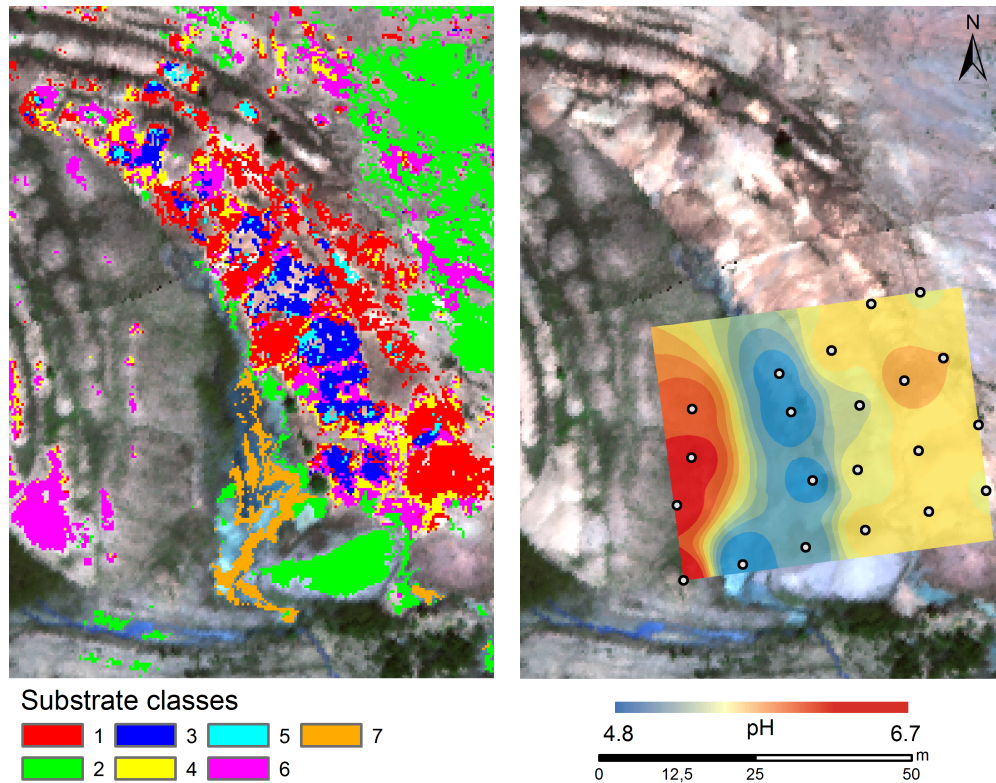


**Figure 6.2** Map of substrate classification obtained from hyper spectral data and pH interpolated from field measurements. Numbers in the left mark type of substrate: 1 – coal clay, 2 – clay of cypris serie yellow, 3 – tuffites, 4 – underlying soils, 5 – kaolinite clay, 6 – clay of cypris serie grey, 7 – jarosite. Scale at the bottom shows pH color coding.

### 6.3.3 Can Near Infrared Spectroscopy Distinguish Between Recent and Fossil Organic Matter in Mine Soils?

To find out if content of recent and fossil organic matter can be predicted from near infrared spectra, predicted values of recent and total organic carbon were compared with their true values (measured by radiocarbon dating and elemental analysis).

Calibration models based only on artificial mixtures could not predict recent nor total organic carbon in soils successfully. However, addition of soil spectra to the calibration improved the predictions considerably – as indicated by root mean square error of cross-validation (RMSECV) and modeling efficiency (EF) comparing explanatory power to model complexity. Models both for recent carbon (RMSECV=0.70, EF=0.95) and total organic carbon (RMSECV=0.85, EF=0.94) were highly successful (Loague & Green 1991; Michel et al. 2009). Parameters of the derived calibrations are similar or better than those reported by other authors who recommend NIRS for measurement of different carbon fractions (Bornemann

et al. 2008; Michel et al. 2009).

The improving effect of soil spectra in calibrations indicates that the spectra of the mixtures and soils differ significantly, i.e. have different spectral features. This is understandable as we may expect that recent organic matter in soils is older and thus more decomposed and fossil organic matter in soils may be modified by weathering and decomposition. The soil samples may be also more variable in mineral composition which may also affect the soil spectra.

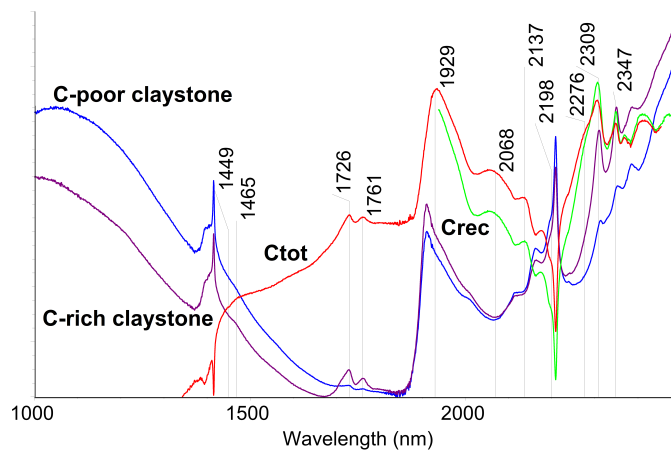


**Figure 6.3** First loading spectra of calibrations for total organic carbon (Ctot) and recent carbon (Crec) together with spectra of C-poor and C-rich claystone.

The most important spectral features for the prediction of recent and total organic carbon are depicted as first loading spectra resulting from partial least square regression (Figure 6.3). The peaks observed can be well assigned to characteristic absorptions of soil organic matter in the near infrared region that have been previously described in literature (Ben-Dor et al. 1997; Michel et al. 2009; Stenberg et al. 2010); their assignments are listed in Table 6.3. For example, it is visible even to naked eye that absorption characteristics of aliphatic structures (1726 and 1761) are more pronounced in C-rich than in C-poor claystone. The same features are visible in the Ctot loading spectrum. This corresponds well with the aliphatic character of fossil organic matter in the studied area, which is mainly kerogen of algal origin (Křibek et al. 1998).

## 6.4 Conclusions

This contribution demonstrates the usefulness of remote sensing techniques in studying post mining sites and at the same time the large potential of these techniques for practical applications.

Classification of overburden substrates brings much better prediction of spatial

**Table 6.3** Band assignment (after Ben Dor et al., 1997; Michel et al., 2009; Stenberg et al., 2010;)

| Wavelength (nm) | Assignment  | Possible constituent                              |
|-----------------|---|---|
| 1449            | $4\nu$ of C=O   | carboxylic acids                                  |
| 1465            | OH in water ( $\nu_2 + \nu_3$ );<br>CH <sub>2</sub>   | cellulose/lignin/starch/<br>pectin                |
| 1582            | OH in water ( $2\nu$ );<br>H-bonded OH group  | pectin/starch/cellulose                           |
| 1726            | $2\nu$ of aliphatic C-H stretch   | cellulose/lignin/starch/<br>pectin/wax/humic acid |
| 1761            | $2\nu$ of aliphatic C-H stretch   | cellulose/lignin/starch/<br>pectin/wax/humic acid |
| 1929            | OH in water ( $\nu_1 + \nu_3$ );<br>$3\nu$ of -C=O and of -COOH,<br>C=O of ketonic carbonyl,<br>CONH <sub>2</sub>                 | cellulose/lignin/glucan/<br>pectin/wax/humic acid |
| 2068            | $3\nu$ of aromatic C=C,<br>COO-hydrogen bond,<br>C=O  | cellulose/glucan/pectin                           |
| 2137            | $3\nu$ of aromatic C=C,<br>COO-hydrogen bond,<br>C=O  | cellulose/glucan/pectin                           |
| 2198            | $3\nu$ of aromatic C=C  | starch/lignin/wax/tannins                         |
| 2276            | combination of O-H stretch<br>and C-O of cellulose;<br>combination of C-H stretch<br>and CH <sub>2</sub> deformation<br>of starch |   |
| 2309            | $3\nu$ of aliphatic C-H,<br>aromatic ring stretch   | humic acid/wax/starch                             |
| 2347            | $3\nu$ of aliphatic C-H   | cellulose/lignin/glucan                           |

distribution of substrate toxicity than interpolation of chemical properties that give best correlation with toxicity from field surveys. There can be a potential to improve the prediction of toxicity by including some auxiliary environmental parameters related to orographic features (e.g. latent drainage system, slope).

Near infrared spectroscopy combined with partial-least squares provides accurate estimates of recent and total organic carbon in mine soil samples. This method may offer a simple, rapid, and low-cost alternative to expensive and time-consuming radiocarbon dating.

### Recommended Reading

- Ben-Dor, E., Chabrilat, S., Dematte, J.A.M., Taylor, G.R., Hill, J., Whiting, M.L. & Sommer, S. 2009. Using Imaging Spectroscopy to study soil properties. *Remote Sensing of Environment* 113: S38–S55.
- Boettinger, J.L., Howell, D.W., Moore, A.C., Hartemink, A.E. & Kienast-Brown, S. 2010. *Digital Soil Mapping*. Springer, 473 p.
- Brady, N.C. & Weil, R.R. 1999. *The nature and properties of soils*. Prentice Hall, Upper Saddle River.
- Mulder, V.L., de Bruin, S., Schaepman, M.E. & Mayr, T.R. 2011. The use of remote sensing in soil and terrain mapping – A review. *Geoderma* 162: 1–19.
- Stenberg, B., Viscarra Rossel, R.A., Mouazen, A.M. & Wetterlind, J. 2010. Chapter Five - Visible and Near Infrared Spectroscopy in Soil Science. *Advances in Agronomy* 107: 163–215.
- Ussiri, D.A.N., Jacinthe, P.-A. & Lal, R. 2014. Methods for determination of coal carbon in reclaimed minesoils: A review. *Geoderma* 214-215: 155–167.